www.embojournal.org

THE EMBO JOURNAL

Structural basis of dynamic glycine receptor clustering by gephyrin

Maria Sola[1,6,7], Vassiliy N Bavro[1,6,8], Joanna Timmins[1,9], Thomas Franz[2], Sylvie Ricard-Blum[3], Guy Schoehn[3,4], Rob WH Ruigrok[4], Ingo Paarmann[5], Taslimarif Saiyed[5], Gregory A O'Sullivan[5], Bertram Schmitt[5], Heinrich Betz[5] and Winfried Weissenhorn[1,*]

[1]European Molecular Biology Laboratory, Grenoble, France, [2]European Molecular Biology Laboratory, Heidelberg, Germany, [3]Institut de Biologie Structurale, Grenoble, France, [4]Laboratoire de Virologie Moléculaire et Structurale, Université Joseph Fourier, Grenoble, France and [5]Max-Planck Institut für Hirnforschung, Frankfurt/Main, Germany

Gephyrin is a bi-functional modular protein involved in molybdenum cofactor biosynthesis and in postsynaptic clustering of inhibitory glycine receptors (GlyRs). Here, we show that full-length gephyrin is a trimer and that its proteolysis *in vitro* causes the spontaneous dimerization of its C-terminal region (gephyrin-E), which binds a GlyR β-subunit-derived peptide with high and low affinity. The crystal structure of the tetra-domain gephyrin-E in complex with the β-peptide bound to domain IV indicates how membrane-embedded GlyRs may interact with subsynaptic gephyrin. *In vitro*, trimeric full-length gephyrin forms a network upon lowering the pH, and this process can be reversed to produce stable full-length dimeric gephyrin. Our data suggest a mechanism by which induced conformational transitions of trimeric gephyrin may generate a reversible postsynaptic scaffold for GlyR recruitment, which allows for dynamic receptor movement in and out of postsynaptic GlyR clusters, and thus for synaptic plasticity.

The EMBO Journal (2004) **23,** 2510–2519. doi:10.1038/sj.emboj.7600256; Published online 17 June 2004
Subject Categories: structural biology; neuroscience
Keywords: gephyrin; gephyrin E-domain; glycine inhibitory receptor; receptor clustering; synaptic plasticity

Introduction

A high concentration and dynamic regulation of receptors in specialized plasma membrane microdomains is crucial for many biological functions including neurotransmission. Efficient synaptic transmission at chemical synapses requires the specific accumulation of neurotransmitter receptors in the postsynaptic plasma membrane domains underlying the transmitter-releasing presynaptic nerve terminals, as reflected by a tight correlation between receptor number and synaptic strength (Nusser *et al*, 1998). Therefore, a highly coordinated process must regulate receptor density in newly established synapses and during their remodeling.

Glycine is a major inhibitory neurotransmitter in the central nervous system (Betz, 1992). Its postsynaptic actions are mediated by inhibitory glycine receptors (GlyRs), which are highly enriched at postsynaptic sites facing glycine-releasing nerve terminals (Betz, 1992). GlyRs are members of a family of ligand-gated ion channels, which includes the closely related gamma-amino butyric acid type A ($GABA_A$) receptors and the more distantly related nicotinic acetylcholine receptors, as well as serotonin type 3 receptors (Moss and Smart, 2001). Postsynaptic GlyR-rich microdomains are stabilized by gephyrin, a peripheral membrane protein that co-purifies with GlyRs (Schmitt *et al*, 1987; Prior *et al*, 1992). In cultured neurons, the postsynaptic accumulation of GlyRs depends on synaptic activity (Kirsch and Betz, 1998; Levi *et al*, 1998) and gephyrin expression (Kirsch *et al*, 1993). Nonsynaptic GlyRs diffuse freely in the plasma membrane, while synaptic GlyRs colocalizing with submembranous gephyrin may alternate within seconds between diffusive and confined states (Meier *et al*, 2001). Thus, gephyrin appears to restrict the plasma membrane mobility of GlyRs. Studies with knockout mice have shown that gephyrin is essential for the postsynaptic clustering of both GlyRs and most $GABA_A$ receptor subtypes (Essrich *et al*, 1998; Feng *et al*, 1998; Kneussel *et al*, 1999a).

At the molecular level, gephyrin acts as a linker between synaptically localized inhibitory receptors and the subsynaptic cytoskeleton (Kirsch and Betz, 1995). GlyR colocalization with gephyrin depends on the large cytoplasmic loop of the receptor β-subunit located between the third and fourth transmembrane segments (Meyer *et al*, 1995; Kneussel *et al*, 1999b). Upon coexpression in non-neuronal cells, gephyrin recruits GlyR β-subunits into intracellular gephyrin aggregates (Kirsch *et al*, 1995), a process that is also observed with $GABA_A$ and NMDA receptors containing a minimal GlyR β-loop binding sequence (Meyer *et al*, 1995; Kins *et al*, 1999; Kneussel *et al*, 1999b). Cytoskeletal anchoring (Kirsch and Betz, 1995) is mediated by an interaction of gephyrin with tubulin (Kirsch *et al*, 1991) and F-actin, and its oligomerization state may be regulated by the gephyrin binding protein collybistin, a GDP–GTP exchange factor (GEF) for GTPases of the Rho/Rac family (Kins *et al*, 2000). Furthermore, profilin and Mena/VASP have been implicated in linking gephyrin

*Corresponding author. European Molecular Biology Laboratory (EMBL), BP 181, 6 rue Jules Horowitz, 38042 Grenoble, France. Tel.: +33 476 207281; Fax: +33 476 207199; E-mail: weissen@embl-grenoble.fr
[6]Both authors contributed equally to this work
[7]Present address: Cristallografia, IBMB-CSIC, Jordi Girona 18-26, 08034 Barcelona, Spain
[8]Present address: Department of Biochemistry, University of Cambridge, 80 Tennis Court Road, Cambridge CB2 1GA, UK
[9]Present address: European Synchrotron Radiation Facility (ESRF), BP 220, 6 rue Jules Horowitz, 38043 Grenoble Cedex 9, France

Received: 3 March 2004; accepted: 5 May 2004; published online: 17 June 2004

and GlyRs to the microfilament system (Mammoto *et al*, 1998; Giesemann *et al*, 2003), and intracellular trafficking of gephyrin may be facilitated by interactions with dynein light-chain (Dlc) subunits of dynein motor protein complexes (Fuhrmann *et al*, 2002).

In addition to functioning as a receptor anchoring protein, gephyrin serves as an enzyme in many tissues. Gephyrin's N-terminal G- (homologous to *Escherichia coli* MogA) and C-terminal E-domains (homologous to *E. coli* MoeA) are involved in a universal molybdenum cofactor (MoCo) biosynthesis pathway, which is conserved from bacteria to humans (Kneussel and Betz, 2000). Like its bacterial homolog MogA, the G-domain from gephyrin forms trimers in solution and in the crystal structure (Liu *et al*, 2000; Sola *et al*, 2001). As both the G- and E-domains of gephyrin have been shown to bind molybdopterin (MPT) (Stallmeyer *et al*, 1999), it has been proposed that gephyrin might be involved in the final steps of molybdenum insertion into MPT (Hasona *et al*, 1998). Notably, hereditary deficiencies in MoCo biosynthesis cause severe brain malformations in humans (Johnson and Wadman, 1995). Whether MoCo biosynthesis and neuronal receptor clustering are two independent functions of gephyrin at the synapse is presently unknown.

Here, we show that full-length gephyrin can adopt different oligomeric states in solution, which may act at distinct steps of synapse formation and modification. Our structural analysis of the E-domain provides insights into how gephyrin interacts with GlyRs and how it mediates GlyR clustering. Together our data suggest how dynamic domain interactions within the gephyrin scaffold may regulate the movement of GlyRs in and out of the synaptic regions during processes such as postsynaptic differentiation and plasticity. Moreover, the conformational transitions of gephyrin reported here might have important implications for the regulation of $GABA_A$ receptors (Essrich *et al*, 1998; Feng *et al*, 1998; Kneussel *et al*, 1999a).

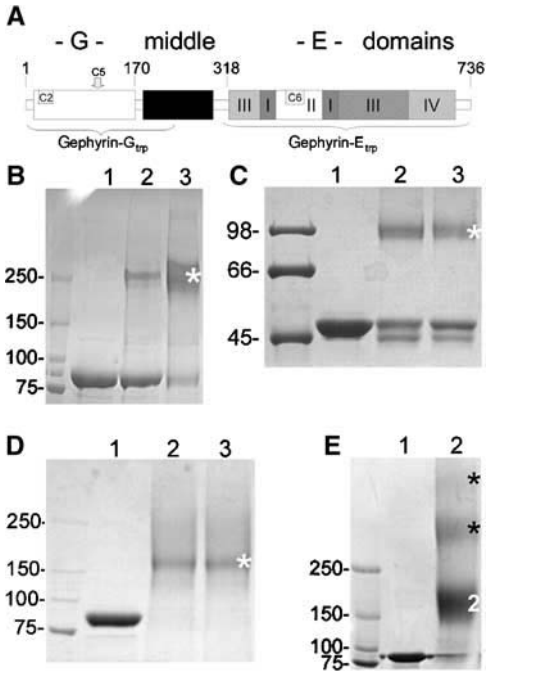

Figure 1 Schematic domain organization and oligomerization of gephyrin. (**A**) Gephyrin consists of an N-terminal G-domain, a middle domain (black box) and a C-terminal E-domain (gray-shaded boxes), composed of four subdomains. The splice cassettes 2 and 6, the position of cassette 5 and tryptic fragments are indicated. (**B**) Chemical crosslinking of gephyrin-300 indicates trimer formation. Lane 1, gephyrin-300; lane 2, gephyrin-300 incubated with 1 mM glutaraldehyde, and lane 3 with 10 mM glutaraldehyde. (**C**) Chemical crosslinking of gephyrin-E shows dimer formation. Lane 1, gephyrin-E; lane 2, gephyrin-E incubated with 1 mM and lane 3 with 5 mM glutaraldehyde. (**D**) Chemical crosslinking of gephyrin-200 reveals dimers. Lane 1, gephyrin-200; lane 2, gephyrin-200 incubated with 1 mM and lane 3 with 5 mM glutaraldehyde. (**E**) Chemical crosslinking of gephyrin-200, which was not yet completely equilibrated into pH 8.0 buffer, reveals dimers (2) and, to a lesser extent, multimers of dimers (asterisks). Lane 1, gephyrin-200; lane 2, gephyrin-200 incubated with 5 mM glutaraldehyde. Final crosslinking products are indicated with an asterisk.

Results

Three different oligomeric states of gephyrin

Purified full-length gephyrin, corresponding to splice variant Ge2,6 (Figure 1A) (Prior *et al*, 1992), eluted from a gel filtration column in a peak corresponding to the size of an ~300 kDa complex (gephyrin-300). Chemical crosslinking of gephyrin-300 produced a new band on SDS–PAGE migrating at ~250 kDa (Figure 1B). This is consistent with a trimeric structure of gephyrin (monomer of 81.3 kDa), and is in agreement with the trimeric crystal structure of the isolated N-terminal G-domain (Sola *et al*, 2001).

Limited proteolysis by trypsin of gephyrin-300 produced three smaller stable fragments, which corresponded to the N-terminal G-domain and part of the intermediate domain (gephyrin-G_{trp}; residues 1–242), and two almost identical fragments of the C-terminal E-domain (gephyrin-E_{trp}; residues 318–736; and 329 (subdomain III) to 736) (Figure 1A), as determined by N-terminal sequencing and mass spectroscopy performed on gephyrin-G_{trp} and gephyrin-E_{trp}. Both C-terminal fragments eluted upon size-exclusion chromatography at a volume corresponding to an ~100 kDa protein (data not shown), indicating dimerization. Indeed, chemical crosslinking of recombinant gephyrin-E (residues 316–736; gephyrin-E) generated an adduct that migrated on SDS–PAGE close to the 98 kDa marker (Figure 1C). Thus, gephyrin-E (apparent molecular weight on SDS–PAGE ~48 kDa; Figure 1C, lane 1) forms dimers in solution, which is consistent with the dimeric structure of the *E. coli* homolog MoeA (Xiang *et al*, 2001). This suggests that gephyrin-E is trapped in a metastable conformation within trimeric gephyrin-300, as its C-terminal E-domain dimerizes spontaneously upon trypsinization.

The ability of gephyrin-E to dimerize upon proteolysis of gephyrin-300 may indicate that, *in vivo*, full-length trimers dimerize via regulated E-domain interactions that trigger gephyrin scaffolding at synaptic sites (Kneussel and Betz, 2000). During attempts to identify mechanisms that may trigger gephyrin clustering, we found that dialysis of gephyrin-300 into an ammonium acetate buffer (pH 6.7) resulted in precipitation. Notably, these precipitates were completely resolubilized by raising the pH from 6.7 to 8.0. Chemical crosslinking of re-solubilized gephyrin produced a novel adduct that migrated on SDS–PAGE slightly above the 150 kDa marker protein, consistent with a dimeric structure (gephyrin-200) (Figure 1D). Variation in the time of back dialysis of ammonium acetate-precipitated gephyrin-300 into

a pH 8 buffer produced a ladder of bands on SDS–PAGE upon chemical crosslinking, whose electrophoretic mobilities were consistent with dimeric, tetrameric and higher order complexes of dimeric gephyrin (Figure 1E). This was confirmed by electrospray ionization mass spectroscopy of ammonium acetate-treated gephyrin-300, which resulted in peaks corresponding to dimers (163 189.0 Da; calculated molecular weight of the monomer 81 302 Da), tetramers (326 410.9 Da) and hexamers (489 599 Da). Equilibrated at pH 8.0, gephyrin-200 was monodisperse as judged by gel filtration (data not shown), consistent with a transition from a trimer to a stable dimer.

Negative staining electron microscopy of low-pH-treated gephyrin-300

Negative staining electron microscopy (EM) of low-pH-treated gephyrin-300 revealed aggregates that appeared to be ordered (data not shown). In an attempt to simulate native trimeric gephyrin binding to membrane-anchored GlyRs, we produced proteoliposomes coated with His–GST–GlyRβ(HR378–426) peptides in complex with gephyrin-300. These proteoliposomes showed clearly visible extensions upon EM analysis (Figure 2A), while control liposomes without gephyrin-300 showed a smooth surface (Figure 2B). When the His–GST–GlyRβ(HR378–426)–gephyrin-300 proteoliposomes were dialyzed against ammonium acetate and then treated with detergent prior to EM analysis, irregular protein networks and loosely organized structures showing spacings of ~10 nm were observed (Figure 2C). After resolubilization at pH 8.0, gephyrin-200 appeared as irregular single particles upon negative staining EM analysis (Figure 2D). Together, these data show that ammonium acetate treatment of gephyrin-300 induced the formation of imperfect gephyrin 'clusters' *in vitro* that can be dissolved to produce dimeric gephyrin-200.

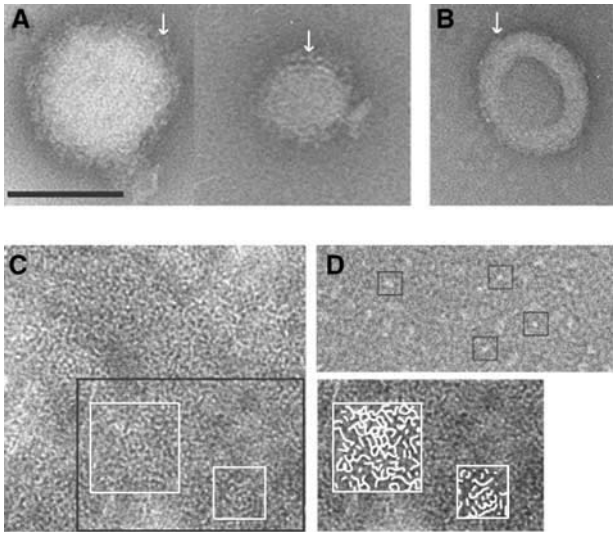

Figure 2 Negative staining EM of 'activated' gephyrin-300. (**A**) Proteoliposomes decorated with complexes formed by His–GST–GlyRβ(HR378–426) and gephyrin-300 (see arrows) (scale bar, 100 nm). (**B**) Control proteoliposomes containing only the His–GST–GlyRβ(HR378–426) fusion protein only. (**C**) Proteoliposomes containing GlyR–gephyrin-300 complexes (as seen in A) were dialyzed against ammonium acetate and liposomes were briefly 'solubilized' in 1% β-octyl glucopyranoside prior to staining with uranylacetate. Network formation is schematically indicated for two areas highlighted by white squares next to panel C. (**D**) Soluble full-length gephyrin-200 shows single irregular particles. Some are indicated by black squares. Panels B–D are shown in the same magnification as indicated in panel A.

Characterization of gephyrin binding to a GlyR β-subunit-derived peptide

Purified gephyrin-300 was incubated with an excess of peptide derived from the cytoplasmic loop of the β-chain of the glycine inhibitory receptor GlyRβ(378–426His) and complexes were separated by gel filtration from free peptide. Co-elution of gephyrin-300 and GlyRβ(378–426His) was confirmed by SDS–PAGE (data not shown) and gephyrin–β-peptide complex formation was further analyzed by native gel electrophoresis. This showed that unliganded gephyrin (Figure 3A, lane 2) migrated substantially faster than gephyrin incubated with increasing amounts of GlyRβ(378–426His) (Figure 3A, lanes 3–7). Furthermore, gephyrin-300–GlyRβ(378–426His) complexes purified by gel filtration (Figure 3A, lane 1) migrated at the same position as fully saturated complexes (Figure 3A, see lanes 1 and 7), indicating that the gephyrin trimer binds GlyRβ(378–426His) with an affinity that is high enough to prevent dissociation during gel filtration. These results are consistent with the tight association of gephyrin with native GlyRs upon affinity purification (Schmitt *et al*, 1987).

We then established that gephyrin-E was sufficient for interaction with the GlyR β-subunit peptide since upon size-exclusion chromatography GlyRβ(378–426) co-eluted with dimeric gephyrin-E (data not shown). In order to estimate peptide occupancy of gephyrin-E, we performed native gel electrophoresis experiments. Gephyrin-E migrated as a single band on a native gel (Figure 3B, lane 1), while the gephyrin-E–GlyRβ(378–426) complex purified by gel filtration (data not shown) produced a band migrating slightly more slowly (Figure 3B, lane 2). Preincubation of gel-filtered gephyrin-E–GlyRβ(378–426) complexes with an approximately five-fold molar excess of free peptide significantly enhanced the band shift, as indicated by a further reduction in electrophoretic mobility of the gephyrin–peptide complex (Figure 3B, lane 3). No band shift was observed with an unrelated peptide (Figure 3B, lane 4). This suggested that gephyrin-E–GlyRβ(378–426) complexes purified by gel filtration chromatography did not exhibit full peptide occupancy.

To further analyze the interaction of gephyrin-E with GlyRβ(378–426), we performed surface plasmon resonance (SPR) measurements. The SPR responses measured at 25°C indicated a clear concentration-dependent binding of gephyrin-E (Figure 3C) and could be fitted to a bivalent analyte model with two distinct binding affinities. The respective affinity constants K_{AB1} and K_{AB2} were found to be in the range of 4×10^{-10}–1.1×10^{-6} M. The large difference in binding affinities between the two binding sites is in agreement with the peptide binding data obtained by gel filtration and native gel analysis. Therefore, our data indicate that gephyrin-E binds two GlyR β-loop peptides with two rather distinct affinities. We propose that this reflects steric hindrance and/or allosteric interactions between the two sites present in the gephyrin-E dimer.

Consistent with this interpretation, a similar differential binding of the GlyR β-peptide was observed for full-length gephyrin-200. Incubation of equimolar ratios of gephyrin-200

and GlyR β-peptide led to a first band shift (Figure 3D, lanes 3 and 4, compared to unliganded gephyrin-200, lane 1) while an excess of GlyRβ(HR378–426) caused a further reduction in electrophoretic mobility (Figure 3D, lane 6). These data are in agreement with gephyrin-200 originating from dimerization of the E-domains, which, as outlined above, contribute differentially to GlyRβ(378–426) binding.

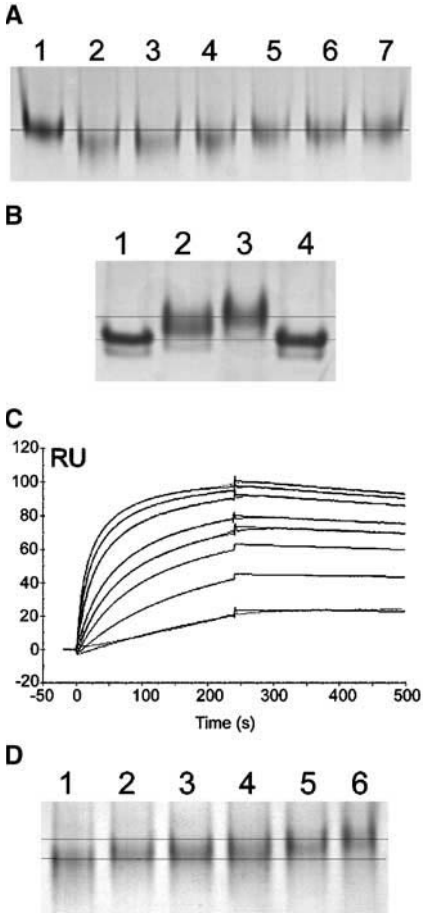

Figure 3 GlyRβ(378–426) peptide interaction with different isoforms of gephyrin. (**A**) Lane 1, native gel electrophoresis of a gephyrin-300–GlyRβ(HR378–426) complex purified by gel filtration; lane 2, gephyrin-300; lanes 3–7, gephyrin-300 was incubated with increasing concentrations of GlyRβ(HR378–426) (lane 5 ~equimolar ratios and lane 7 a five-fold molar excess of peptide); the shift in mobility is the same in lanes 1 and 7 (see line), indicating that gephyrin-300 binds GlyRβ(HR378–426) with 'high' affinity, which allows purification of a fully saturated complex by gel filtration. (**B**) Gephyrin-E binds GlyRβ(378–426) with two different affinities. Lane 1, gephyrin-E; lane 2, gephyrin in complex with GlyRβ(378–426) as co-eluted from a superdex-200 gel filtration column; lane 3, gephyrin-E incubated with a five-fold molar excess of GlyRβ(378–426), which leads to a further band shift as indicated by the two lines; lane 4, gephyrin-E incubated with an unrelated control peptide. (**C**) Binding of gephyrin-E to immobilized GlyRβ(HR378–426) peptides as assayed by SPR. The experimental sensorgrams derived from increasing gephyrin concentrations (1–40 nM) were best fitted to a bivalent analyte model with excellent χ^2 values (<0.5) for the whole concentration range. Experimental curves are shown with the fitted ones overlaid. (**D**) Gephyrin-200 binds GlyRβ(HR378–426) with two different affinities. Lane 1, gephyrin-200; lanes 2–6, complexes formed by adding increasing concentrations of GlyRβ(HR378–426) (lane 3 ~equimolar ratios and lane 6 a five-fold molar excess of GlyRβ). The two proposed binding steps are indicated by two lines that represent bands before binding and a fully saturated complex, while intermediate forms migrate in between.

Crystal structure of dimeric gephyrin-E in complex with a GlyR peptide

Gephyrin-E–GlyRβ(378–426) complexes purified by gel filtration produced diffraction quality crystals, while gephyrin-E completely saturated with GlyRβ(378–426) (see Figure 3B, lane 3) did not crystallize. The crystal structure of the complexes obtained by gel filtration revealed a dimeric molecule composed of two pseudosymmetrically arranged monomers. The structure of the gephyrin-E monomer within this dimer is L-shaped and composed of domains I, II, III and IV (Figure 4A). At the N-terminus a short helical segment (alpha1) packs within domain III, but is quickly followed by domain I, whose four β-strands and two helices constitute a small core that together with the following extended main chain forms a bridge between domains III and II. Within the dimer, domain II is rather flexibly linked as indicated by its slightly different orientation (Figure 4B) and is composed of a central four-stranded β-sheet and several extensive loops. From domain II the chain follows an antiparallel extended path toward domain I and subsequently to domain III. The

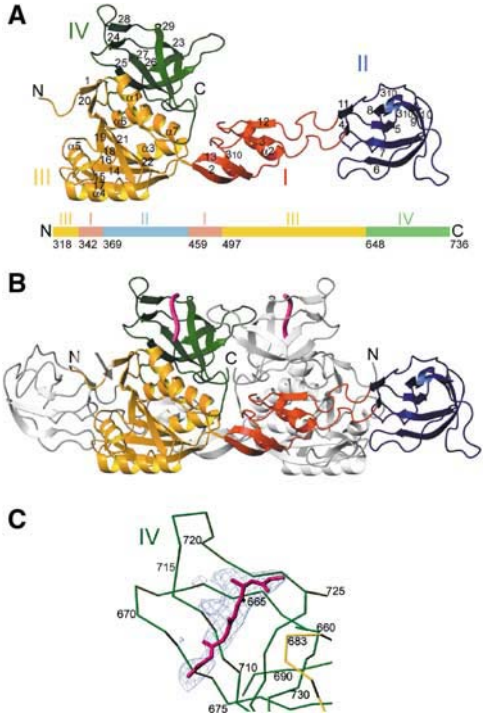

Figure 4 Crystal structure of gephyrin-E in complex with GlyRβ(378–426). (**A**) Ribbon diagram of the monomer showing the four subdomains I, II, III and IV. The secondary structure elements are labeled (β-strands as numbers, alpha helices as α1, etc. and 3/10 helices as 3/10). The N-terminus starts at residue 318 and the C-terminal end comprises residue 736. The representation of the individual domains in the linear sequence is shown schematically underneath. (**B**) Ribbon diagram of the gephyrin-E dimer; one monomer is shown with the same domain colors as in panel A and the second one is shown in white. GlyR peptide bound to domain IV is shown in magenta. Dimerization buries the C-terminal ends at the interface of domains IV and IV′, while the N-terminus is freely accessible to connect to the intermediate domain. The position of the proposed MPT binding site constituted by domains II and III′ is indicated by an arrow. (**C**) Close-up of the position of extra electron density (F_o–F_c omit map; 2.5 sigma cutoff) accounting for a partial GlyR peptide model. The poly-Ala model (shown in magenta) could potentially be a GlyR peptide-derived β-strand that runs parallel to β 26 of domain IV.

latter displays an alpha/beta arrangement composed of a central β-sheet surrounded by α-helices on both sides. Finally, domain III connects to domain IV, which forms the upper part of the L-shape and consists of five antiparallel β-strands with two parallel extended loops that contain two additional β-strands (Figure 4A). Domain IV also harbors the proposed GlyRβ(378–426) peptide binding sites (Figure 4B).

GlyR β-peptide binding site of gephyrin-E

An F_o–F_c omit electron density map contoured at 2.5 sigma revealed extra electron density in a depression located between β-strands 25, 27, 28, 29 and their connecting loops (Figure 4C). The density is positioned parallel to β29 and perpendicular to β27 and extends into both directions (visible at a lower σ cutoff). Although the extra electron density was continuous in one monomer, the second monomer only showed clusters of electron density at the corresponding position. The connected electron density was of insufficient quality to identify sequence patterns but accommodated a modeled six residue-long Ala–Gly peptide, which could represent a short β-strand that corresponds to a section of the GlyRβ(378–426) peptide present in the complex crystallized. The poor quality of the electron density most likely reflects a reduced occupancy of the GlyRβ(378–426) binding site in our crystals (see Figure 3B). In addition, the crystals could be only cryo-protected in 2.5 M Li_2SO_4, which further decreased the peptide binding, as detected by SDS–PAGE analysis of crystals after different soaking times (data not shown).

Confirmation of the proposed GlyR β binding site

In order to confirm the crystallographically determined position of GlyRβ(378–426) binding, we substituted the sequence of the nonconserved loop region connecting β-strands 27 and 28 (residues 713–721) by that of MoeA, which is shorter by three residues. The resulting gephyrin-E mutant (gephyrin-E_{mut}) no longer bound GlyRβ(378–426) peptides, as revealed by native gel electrophoresis where incubation of gephyrin-E_{mut} with a molar excess of GlyRβ(378–426HIS) produced no change in mobility (Figure 5A, lanes 1–3). In contrast, native gephyrin-E showed a clear band shift under identical conditions (Figure 5A, lanes 4–6; similar to Figure 3B). Gephyrin-E_{mut} eluted at the same position from a gel filtration column as native gephyrin-E and could be crosslinked to a dimer as found for wild-type gephyrin-E (Figure 5B), indicating that the loop replacement did not alter the overall behavior of the protein. Finally, upon heterologous expression in HEK 293 cells, full-length gephyrin$_{mut}$ failed to recruit a DsRed–GlyRβ(378–426) fusion protein to gephyrin-rich intracellular domains (Figure 5C), a property that is characteristic of wild-type gephyrin as indicated by the colocalization of gephyrin and GlyRβ fusion proteins in intracellular aggregates (Figure 5D) (Meyer *et al*, 1995; Kneussel *et al*, 1999b). Complementary results were obtained in pull-down experiments with mutated full-length gephyrin (gephyrin$_{mut}$), which showed that the GlyRβ–GST fusion protein was able to pull down native gephyrin but not gephyrin$_{mut}$ (Figure 5E, lanes 2 and 4). Notably, under the same conditions, interaction of Dlc with both native gephyrin and gephyrin$_{mut}$ was unchanged (Figure 5E, lanes 3 and 6). Thus, loop 713–721 is important for GlyR(378–426) binding *in vitro* and *in vivo*, as indicated by the crystal structure.

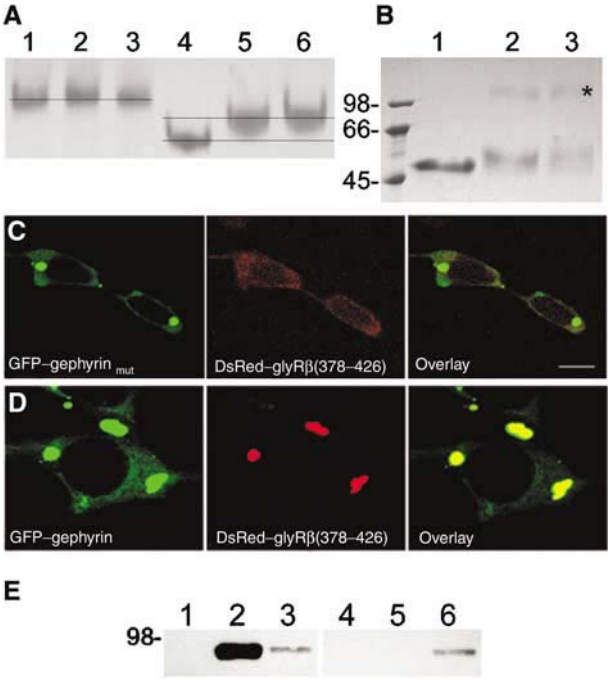

Figure 5 A gephyrin mutant that does not bind GlyRβ peptides. (**A**) Gephyrin-E_{mut} did not bind GlyRβ(HR378–426). Native gel electrophoresis of gephyrin-E_{mut}–GlyR complexes compared to native gephyrin-E–GlyR complexes. Lane 1, gephyrin-E_{mut}; lane 2 gephyrin-E_{mut} incubated with equimolar and lane 3 with a five-fold molar excess of GlyRβ(HR378–426) peptide. Lane 4, gephyrin-E; lanes 5 and 6, gephyrin-E–GlyRβ(HR378–426) complexes (equimolar amounts and a five-fold molar excess, respectively). Note that unliganded gephyrin-E_{mut} migrates in a different manner compared to wild-type gephyrin-E due to the loop exchange. Similar band positions are indicated by lines. (**B**) Chemical crosslinking of gephyrin-E_{mut} results in the same dimer as obtained with wild-type gephyrin-E. Lane 1, gephyrin-E_{mut}; lanes 2 and 3, gephyrin-E_{mut} crosslinked with 1 and 10 mM EGS, respectively. (**C**, **D**) HEK 293 cells were cotransfected with DsRed–GlyRβ(378–426) and GFP–gephyrin$_{mut}$ (C) or wild-type GFP–gephyrin (D). Colocalization is indicated by the yellow color in the overlay. Occasionally, DsRed–GlyRβ(378–426) is also found in the nucleus, as previously observed (Kneussel *et al*, 1999b). Scale bar, 8 μm. (**E**) Pull-down of full-length gephyrin and gephyrin$_{mut}$. Full-length gephyrin pull-down with GST (lane1), GST–GlyRβ(378–426) (lane 2) and GST–Dlc (lane 3). Full-length gephyrin$_{mut}$ pull-down with GST (lane 4), GST–GlyRβ(378–426) (lane 5) and GST–Dlc (lane 6).

Structure of the gephyrin-E dimer interface and sequence conservation

Dimerization of gephyrin-E has been proposed to be important for enzymatic activity as well as for receptor clustering (Kneussel and Betz, 2000; Xiang *et al*, 2001). The crystal structure of gephyrin-E reveals that the dimer (monomers A and B) is stabilized primarily by an antiparallel packing of domains I and III against the same domains I′ and III′ of the symmetry-related monomer. Domains IV and IV′, which are related by a two-fold axis, also participate in dimer formation, while domains II and II′ extend from the core (Figure 4B). The dimer interface buries a large surface of 3610 Å^2 and is dominated by polar interactions with contributions from van der Waals contacts. Notably, although mammalian gephyrin-E and *E. coli* MoeA display 45% sequence similarity, most dimer–dimer interactions are mediated by nonconserved residues (Figure 6A and B).

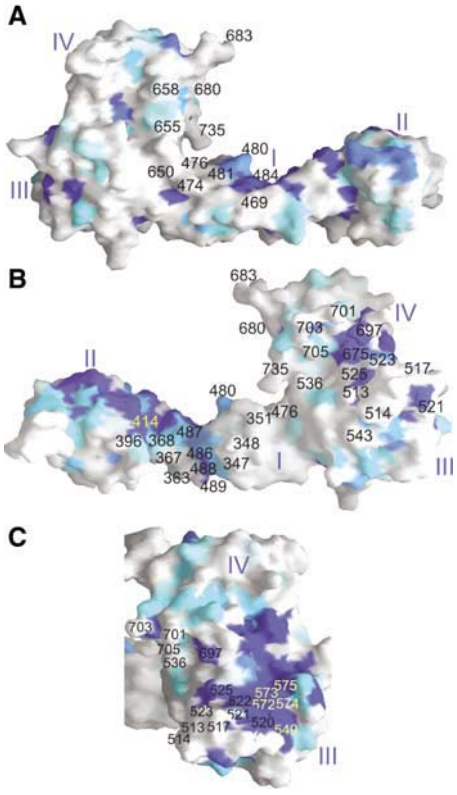

Figure 6 Dimer interface analysis and sequence conservation. (**A**) Sequence conservation was mapped onto the surface of monomeric gephyrin-E based on the alignment of sequences from gephyrin-E from *R. norvegicus*, gephyrin from *Gallus gallus*, cinnamon E-domain from *Drosophila melanogaster*, Moco-1 E-domain from *Caenorhabditis elegans*, the Cnx1 E-domain from *Arabidopsis thaliana*, CnxE from *Aspergillus nidulans* and MoeA from *E. coli*. Conserved residues are shown in blue and conservative changes in light blue; white, no homology. Residues involved in dimer contacts are labeled. (**B**) same as (A) but rotated by 180°. (**C**) Close-up of a major surface sequence conservation patch at domain III. Residues implicated in MPT binding (Asp549) and catalysis (residues 572–575) are shown in yellow.

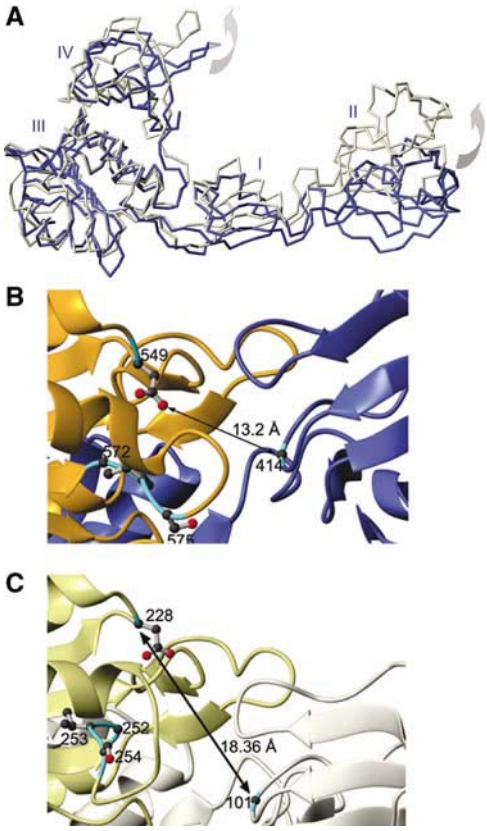

Figure 7 Comparision of gephyrin-E and the *E. coli* MoeA structure. (**A**) Superposition of C-alpha atoms of one gephyrin-E monomer and one MoeA monomer (Xiang *et al*, 2001). The r.m.s.d. between the two monomers is 4.2 Å. (**B**, **C**) The movement of domain II leads to a more closed conformation of gephyrin-E with respect to the putative active site when compared to MoeA. This positions MPT binding residues Gly414 closer to Asp549 (B) than the corresponding residues Gly101 and Asp228 from MoeA (C). The corresponding monomers in panels B and C are shown as ribbon diagrams in different colors and the residues implicated in catalysis are shown as a ball and stick model.

Similarly, sequence conservation between surface residues is only limited and confined to larger surface patches on domains II and III (Figure 6B and C). Residues from these domains have been proposed to constitute the proposed active site positioned at the interface of domains II and III′ (Xiang *et al*, 2001). Specifically, residues Gly414 (domain II; Figure 6B) and Asp549 (domain III′; Figure 6C) have been implicated by mutagenesis in MPT binding (Heck *et al*, 2002) and the conserved sequence 572–GGVS–575 (Figure 6C) has been suggested to be important for the enzymatic activity of E-domains (Schwarz *et al*, 2000; Xiang *et al*, 2001).

Superpositioning of the C-alpha atoms of bacterial MoeA (pdb 1g8r) and gephyrin-E reveals an overall similar structure and an r.m.s.d. of 4.2 Å (Figure 7A). Main differences are due to movements of domains IV and II, which result in a slight rotation of domain IV and an ∼20 Å displacement of domain II (Figure 7A). The movement of domain II might play a role in the catalytic activity, as a transition of the cleft between domains II and III′ from a 'closed' conformation as seen in gephyrin-E to a more open conformation as found in MoeA might influence MPT binding. Notably, this would reduce the distance between active site residues Asp549 and Gly414 to ∼13 Å (Figure 7B) as compared to a distance of ∼18 Å in the case of the homologous MoeA residues (Figure 7C) (Schwarz *et al*, 2000; Xiang *et al*, 2001; Heck *et al*, 2002).

Discussion

In this work, we present the crystal structure of gephyrin-E and evidence that full-length gephyrin can exist in three different oligomeric states: trimers (gephyrin-300), 'aggregates' and dimeric gephyrin (gephyrin-200), which all bind a peptide derived from the GlyR β-subunit. We further confirm that the E-domain of gephyrin is sufficient for the GlyR interaction (Rees *et al*, 2003; Schrader *et al*, 2004), a result that is in contrast to the proposal that splice cassette 5 located within the G-domain (Figure 1A) is involved in GlyR recognition (Meier *et al*, 2000; Meier and Grantyn, 2004).

Structural comparison of gephyrin-E and MoeA

The crystal structure of gephyrin-E reveals a dimer that is composed of four subdomains, as shown for its bacterial homolog MoeA (Xiang *et al*, 2001). Due to their conserved function in MoCo biosynthesis, the overall structures of gephyrin-E and bacterial MoeA are highly similar. The main structural differences are due to movements of domains IV

and II. Conformational flexibility of domain II might be important for its enzymatic activity, which locates to a cleft formed by domains II and III′ (Schwarz *et al*, 2000; Xiang *et al*, 2001; Heck *et al*, 2002) as it might allow for 'close' and 'open' conformations of the active site cleft. Closure would bring residues Gly414 and Asp549 (gephyrin domain II) as well as conserved residues 573–575 (domain III′), all implicated in MPT binding and catalytic activity, into close proximity (Schwarz *et al*, 2000; Xiang *et al*, 2001; Heck *et al*, 2002). Stallmeyer *et al* (1999) have speculated that such conformational flexibility could account for the cooperativity of MPT binding, which might contribute to an allosteric mechanism of MoeA function (Xiang *et al*, 2001). The proposed flexibility is also consistent with the two slightly different conformations of both domains II and II′ within our gephyrin-E dimer structure.

GlyR β-peptide interaction with gephyrin

The gephyrin GlyR receptor interaction (Schmitt *et al*, 1987; Prior *et al*, 1992) has been previously mapped to 49 amino acids of the cytoplasmic loop connecting the third and the fourth transmembrane domains of the β-subunit (Meyer *et al*, 1995; Kneussel *et al*, 1999b). Gel filtration chromatography, native gel electrophoresis and SPR experiments suggest that full-length gephyrin-300 binds GlyR β-subunit peptides with high affinity while the dimers gephyrin-200 and gephyrin-E display both high-affinity binding (such as nanomolar binding and complex identification by gel filtration) and low-affinity binding (in the micromolar range and dissociation under gel filtration). Dual-affinity binding of a GlyR β-peptide to gephyrin-E has recently also been reported by Schrader *et al* (2004); however, the K_D's derived from our SPR experiments and their isothermal titration calorimetry measurements differ, which might be attributed to substantial differences in experimental setups (see Schrader *et al*, 2004).

Our experiments suggest that dimerization of the E-domain transforms one high-affinity site into a low-affinity one, probably due to steric hindrance. Notably, the crystal structure showed low occupancy by GlyR β-subunit peptide, since only gel-filtered complexes could be crystallized. In addition, cryo-protection of the crystals required high salt, which might have further reduced GlyR β-peptide binding. Although the structure of the gephyrin-E GlyR β-subunit complex reveals electron density that could be attributed to the β-subunit peptide bound to domain IV, we used mutagenesis analyses to corroborate the localization of the GlyR β-peptide binding site for both the E-domain dimer and full-length gephyrin. The position of the binding site indicates that the E-domain acquired the additional GlyR binding function by insertion of β-strand 28 as part of a longer loop connecting β-strands 27 and 29, which is not found in MoeA (Xiang *et al*, 2001). Interestingly, the peptide binding site identified here is ideally positioned to allow interaction of the E-domain dimer with membrane-anchored GlyRs (Figure 8A), which is consistent with the proposal that E-domain dimerization is involved in receptor clustering (Kneussel and Betz, 2000; Xiang *et al*, 2001).

E-domain monomer/trimer to dimer transition

In gephyrin-300, the E-domain should be contained as a monomer within the trimeric structure. This implies that E-domain dimerization must be prevented either by a conformation that differs from that observed in the crystal structure, or by masking the dimerization interface through interactions with the intermediate domain. In addition, a limited sequence conservation as observed at the dimer interface has been generally predicted to be common to proteins that form transient oligomers (Nooren and Thornton, 2003). Our data suggest that the E-domain is in a metastable conformation within native gephyrin-300. Hence, a regulated removal of specific trimerization constraints appears to be required for dimerization. *In vitro*, this can be achieved by proteolysis or ammonium acetate treatment. *In vivo*, a specific, yet unknown signal might trigger the conformational rearrangements that induce(s) E-domain dimerization.

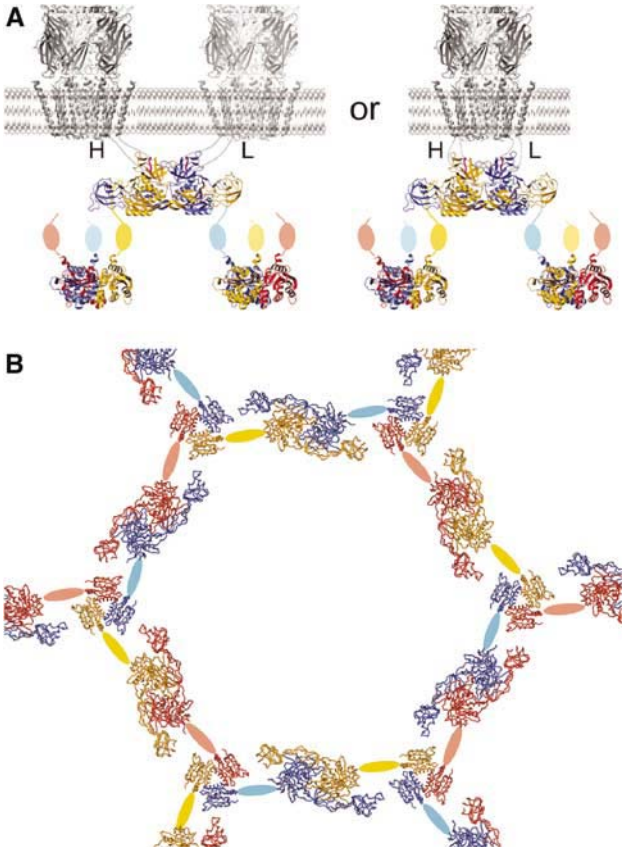

Figure 8 Model for network formation and GlyR docking by gephyrin-300. (**A**) The E-domain dimer might either interact with β-subunits from two different GlyR receptors (left panel) or with two β-subunits derived from one GlyR receptor (right panel). High- and low-affinity interactions with GlyR β-subunits are indicated (H, L). (**B**) E-domain dimerization could potentially form a hexagonal network as viewed from the top. The G- and E-domains are shown as ribbon and the intermediate domain is drawn schematically. Each monomer chain is color coded differently.

Network formation of gephyrin in vitro

E-domain dimerization has been proposed to cause clustering of GlyRs by forming a gephyrin scaffold (Kneussel and Betz, 2000; Xiang *et al*, 2001). Our *in vitro* data show that gephyrin-300 can be 'activated' to form a protein network with no defined higher order by lowering the pH from 8.0 to 6.7. The lack of symmetry seen in EM might be due to the absence of correct anchors both to the membrane and/or the cytoskeleton (Kirsch and Betz, 1995; Kneussel and Betz, 2000).

However, as the three-fold symmetry axis of the G-domain and the two-fold symmetry axis of the E-domain have to be related by a fixed angle to generate the hypothesized hexagonal network (Kneussel and Betz, 2000), internal flexibility might prevent ordered polymerization resulting in an 'open' network with multiple shapes as observed here.

Unexpectedly, pH shift induced disassembly of the network formed *in vitro* and produced dimeric gephyrin-200, as confirmed by mass spectroscopy, which implies that the N-terminal G-domain trimer (Sola *et al* 2001) can disassemble under close to physiological conditions.

Implications for dynamic GlyR clustering

Based on these findings, we propose the following model for gephyrin scaffolding at the synapse (Figure 8). In the cytosol, gephyrin folds into a trimeric conformation, which is metastable and prevents dimerization of the E-domains. Via its E-domains gephyrin-300 can bind to membrane-anchored GlyRs, which are either contained in transport vesicles (Hanus *et al*, 2004) or have been randomly inserted into the neuronal somatodendritic membrane (Rosenberg *et al*, 2001). A yet unknown signal such as phosphorylation or acylation then triggers a conformational change of gephyrin-300 that initiates the dimerization of E-domains belonging to different trimers (Figure 8A). E-domain dimerization also creates two adjacent GlyR β-subunit binding sites, of which one displays only low affinity. As heteromeric GlyRs contain multiple copies of the β-subunit (Moss and Smart, 2001) (J Grudzinska, H Betz and B Laube, unpublished data), this low-affinity site might recruit a free β-subunit loop region from an already prebound GlyR, and thus contribute to the stability of the submembranous gephyrin lattice through GlyR-mediated crosslinking of the E-domain dimer. Due to the length of the cytoplasmic GlyR β-subunit M3–M4 loop region (~100 amino acids), dimeric gephyrin-E might either dock onto two β-chains derived from two different GlyRs or onto two β-chains within one pentameric GlyR (Figure 8A). E-domain dimerization then leads to the formation of a submembranous gephyrin network, which might be hexagonal as previously suggested (Figure 8B) (Kirsch and Betz, 1995) or more loosely organized as indicated by our *in vitro* data (Figure 2C).

In order to enable dynamic changes of the postsynaptic specialization, disassembly of the gephyrin scaffold must also occur. Single receptor tracking has identified three major GlyR pools in differentiating neurons that have distinct diffusion properties: mobile extrasynaptic receptors that are not associated with gephyrin, less mobile perisynaptic receptors that may have gephyrin bound and slowly diffusing synaptic receptors anchored to the gephyrin scaffold (Dahan *et al*, 2003). Notably, rapid dynamic exchanges are seen between these receptor pools, in agreement with previous studies that postulated that GlyRs are clustered by a diffusion-trap mechanism during synaptogenesis (Kirsch and Betz, 1998; Levi *et al*, 1998). Our *in vitro* data suggest that disassembly of the gephyrin lattice might produce gephyrin-200, which is dimeric most likely due to E-domain dimerization. In this case, the N-terminal trimeric G-domains must disassemble for network opening and GlyR release from synaptic sites. Disassembly of the gephyrin scaffold might be further facilitated by one of the E-domain interactions with GlyR β-loop sequences being of only low affinity. As a result, mobile gephyrin-200–GlyR complexes that could be endocytosed or move laterally out of the postsynaptic membrane would be generated. On the other hand, newly assembled gephyrin-300–GlyR complexes may enter the synapse and participate in receptor clustering. In conclusion, we propose that conformational transitions of gephyrin regulate both its assembly state and its interactions with inhibitory receptors, and thereby allow for a dynamic regulation of receptor density during synapse formation, modification and elimination.

Materials and methods

Expression vectors

The cDNA encoding full-length gephyrin (amino acids 1–736) from *Rattus norvegicus* (Swissprot Q03555) was cloned into the pRSET expression vector (Invitrogen) using *Nhe*I and *Hin*dIII sites and expressed as an N-terminally 6-His-tagged recombinant protein. cDNA fragment corresponding to residues 316–736 was subcloned into a modified pMAL-c2g vector (New England Biolabs) containing a TEV protease cleavage site and into pRSET. In full-length gephyrin$_{mut}$ and gephyrin-E$_{mut}$, residues 713–721 (PPKTEQYVE) were replaced by the corresponding residues of *E. coli* MoeA (ERDRGN) by using a standard PCR mutagenesis protocol and cloned into pRSET using *Nhe*I and *Hin*dIII restriction sites.

A cDNA fragment encoding residues 378–426 (49 amino acids) (Meyer *et al*, 1995) of the GlyR β-subunit was subcloned into the modified pMAL-c2g-TEV vector and a pETM30 vector (EMBL-Heidelberg, Protein Expression Facility). The pETM30 constructs were further modified to contain either a C-terminal 6-His tag, GlyRβ(378–426His), or two extra N-terminal residues (His, Arg), GlyRβ(HR378–426). The sequences of all expression constructs were confirmed by DNA sequencing.

Protein expression and purification

Protein expression was performed in *E. coli* strains BL21 codon plus™ (Invitrogen) and BL21 (DE3) pLysS (Novagen). Recombinant proteins were purified on an Ni^{2+} affinity matrix, amylose resin or on glutathione agarose as described (Supplementary data). Expression of gephyrin constructs in mammalian (HEK) 293 cells was performed as described (Kneussel *et al*, 1999b; Fuhrmann *et al*, 2002). The conditions for the GST pull-down are described elsewhere (Supplementary data).

Limited proteolysis of full-length gephyrin

A 1 mg portion of full-length gephyrin-300 was treated with trypsin at a 1:500 (w/w) ratio and the reaction was stopped with 1 mM PMSF. The resulting fragments were analyzed by N-terminal sequencing and mass spectroscopy.

Crosslinking of gephyrin oligomers

Samples (buffer D, 50 mM Hepes (pH 8.0), 100 mM NaCl, 20 mM β-mercaptoethanol) were incubated at room temperature for 20 min with glutaraldehyde concentrations as indicated. Gephyrin-E$_{mut}$ was crosslinked with ethylene glycol bis[succinimidyl succinate] (EGS) in buffer D (without β-mercaptoethanol) and reactions were quenched by adding Tris (pH 8.0) to a final concentration of 50 mM.

Gephyrin–GlyR peptide complex formation

Gephyrin-300, gephyrin-200, gephyrin-E and gephyrin-E$_{mut}$ were incubated with increasing amounts of either purified GlyRβ(378–426) or GlyRβ(HR378–426) peptides (molar ratios up to 1:5) as indicated on ice for 1 h. Gephyrin-E was also incubated with an unrelated control peptide (YTSLIHSLIEESQNQQEKNEQELLELDKWASLWNWF). The mobility of the complexes was analyzed by either 9 or 7% nondenaturing polyacrylamide gel electrophoresis.

Surface plasmon resonance

SPR measurements were performed at 25°C on a BIAcore 3000 (BIACORE AB, Uppsala, Sweden) as described (Supplementary data).

Ammonium acetate (pH 6.7) treatment of gephyrin-300 in vitro

Gephyrin-300 (1 mg/ml) purified from gel filtration was dialyzed against 50 mM ammonium acetate (pH 6.7) and 20 mM β-mercaptoethanol. Precipitation was visualized after 3–4 h and the dialysis buffer was exchanged against buffer D and further dialyzed until the solution was clear again (>30 min).

'Native' mass spectroscopy

The measurements were carried out on an ESI-Q-Tof2 instrument (Micromass, Manchester, UK) under native like conditions (100 mM ammonium acetate). MassLynx software (Micromass) was used for the deconvolution analysis.

Preparation of liposomes coated with dimeric GlyR peptides and gephyrin-300

Liposomes containing 20% (w/v) 1,2-dioleoyl-sn-glycero-3-[*N*-(5-amino-1-carboxypentyl)iminodiacetic acid)succinyl (DOGS-NTA) (Avanti Polar Lipids), 75% (w/v) phosphatidylcholine (Sigma) and 0.5% cholesterol (w/v) (Sigma) were produced as described (Supplementary data).

Electron microscopy of gephyrin

Samples were applied to the clean side of carbon on mica (carbon/mica interface) and negatively stained with either 1% uranyl acetate (gephyrin-200; proteoliposomes after ammonium acetate treatment) or 1% sodium silicotungstate (proteoliposomes coated with either His–GST–GlyRβ(HR378–426) or His–GST–GlyRβ(HR378–426)–gephyrin-300 as described (Supplementary data).

Crystallization of gephyrin-E in complex with GlyRβ(378–426)

Crystals of gephyrin-E in complex with GlyRβ(378–426) (in 20 mM Tris (pH 8), 100 mM NaCl, 25 mM β-mercaptoethanol at 7.5 mg/ml) were obtained by mixing 1 µl of reservoir buffer (1 M Li_2SO_4, 10 mM $MgCl_2$, 50 mM Na-cacodylate (pH 6.0)) with 1 µl of protein solution. For cryoprotection, the crystals were gradually (200 mM steps, 20 min each) transferred into the well buffer adjusted to 2.5 M Li_2SO_4.

Data collection, structure solution and refinement

Diffraction data were collected at the European Synchrotron Radiation Facility (Grenoble, France) at beam line ID14-EH2. The data were processed using the programs Mosflm and SCALA (CCP4, 1994) (see Table I). The structure was solved by molecular replacement as described (Supplementary data).

The final model was refined to an *R*-factor of 25.0 and an R_{free} of 30.4. The model exhibits good stereochemistry (Table I) and 98% of the residues are in most favored and additionally allowed regions according to the Ramachandran plot as defined in PROCHECK (Laskowsky *et al*, 1993). Monomer A consists of residues 318–574, 580–697 and 700–736 (side chains of residues 318, 319, 580, 695–697 and 736 were modeled as alanines) and monomer B contains residues 318–430 and 445–736 (residues 318, 319, 445–447 and 736 were modeled as alanine). In addition, eight sulfate ions were included in the refinement. For structure analysis, see Supplementary data. The coordinates have been deposited in the RCSB Protein Data Bank (accession code 1T3E).

Table I Data collection and refinement statistics

Space group	P61
Cell constants	$a = b = 161.6$, $c = 126.2$
Wavelength (lambda in Å)	0.933
Whole resolution range (last shell) (Å)	30–3.25 (3.4–3.25)
No. of measurements	84 498 (11 074)
No. of unique reflections	28 617 (4201)
R_{merge} (%)[b]	10.8 (49.4)
Completeness (%)	97.1 (97.8)
$\langle I/\mathrm{sigma}(I) \rangle$ (%)	7.8 (1.6)
Resolution range used for refinement (Å)	30–3.25
No. of reflections (working set/test set)	27 163/1446
R_{factor}/free R_{factor}	24.4/30.4
No. of protein atoms	6184
No. of sulfates	8
R.m.s.d. from target values	
Bonds (Å)	0.009
Angles (deg)	1.232

Supplementary data

Supplementary data are available at *The EMBO Journal* Online.

Acknowledgements

We thank Silke Fuchs for technical assistance. This work was supported by EMBL (WW), Deutsche Forschungsgemeinschaft (SFB 628) and 'Fonds der Chemischen Industrie' (HB). VB was supported by a predoctoral fellowship from the 'Louis-Jeantet Fondation de Medicine' and MS and GAO'S were both supported by a Marie Curie fellowship from the European Union.

References

Betz H (1992) Structure and function of inhibitory glycine receptors. *Q Rev Biophys* **25:** 381–394

Dahan M, Levi S, Luccardini C, Rostain P, Riveau B, Triller A (2003) Diffusion dynamics of glycine receptors revealed by single-quantum dot tracking. *Science* **302:** 442–445

Essrich C, Lorez M, Benson JA, Fritschy JM, Luscher B (1998) Postsynaptic clustering of major GABAA receptor subtypes requires the gamma 2 subunit and gephyrin. *Nat Neurosci* **1:** 563–571

Feng G, Tintrup H, Kirsch J, Nichol MC, Kuhse J, Betz H, Sanes JR (1998) Dual requirement for gephyrin in glycine receptor clustering and molybdoenzyme activity. *Science* **282:** 1321–1324

Fuhrmann JC, Kins S, Rostaing P, El_Far O, Kirsch J, Sheng M, Triller A, Betz H, Kneussel M. (2002) Gephyrin interacts with Dynein light chains 1 and 2, components of motor protein complexes. *J Neurosci* **22:** 5393–5402

Giesemann T, Schwarz G, Nawrotzki R, Berhorster K, Rothkegel M, Schluter K, Schrader N, Schindelin H, Mendel RR, Kirsch J, Jockusch BM (2003) Complex formation between the postsynaptic scaffolding protein gephyrin, profilin, and Mena: a possible link to the microfilament system. *J Neurosci* **23:** 8330–8339

Hanus C, Vannier C, Triller A (2004) Intracellular association of glycine receptor with gephyrin increases its plasma membrane accumulation rate. *J Neurosci* **24:** 1119–1128

Hasona A, Ray, RM, Shanmugam KT (1998) Physiological and genetic analyses leading to identification of a biochemical role for the moeA (molybdate metabolism) gene product in *Escherichia coli*. *J Bacteriol* **180:** 1466–1472

Heck IS, Schrag JD, Sloan J, Millar LJ, Kanan G, Kinghorn JR, Unkles SE (2002) Mutational analysis of the gephyrin-related molybdenum cofactor biosynthetic gene *cnxE* from the lower eukaryote *Aspergillus nidulans*. *Genetics* **161:** 623–632

Johnson JL, Wadman SK (1995) Molybdenum cofactor deficiency and isolated sulfite oxidase deficiency. In *The Metabolic and Molecular Bases of Inherited Diseases*, Scriver CR, Beaudet AL, Sly WS, Valle D (eds) 7th edn, pp 2271–2283. New York; McGraw-Hill

Kins S, Betz H, Kirsch J (2000) Collybistin, a newly identified brain-specific GEF, induces submembrane clustering of gephyrin. *Nat Neurosci* **3:** 22–29

Kins S, Kuhse J, Laube B, Betz H, Kirsch J (1999) Incorporation of a gephyrin-binding motif targets NMDA receptors to gephyrin-rich domains in HEK 293 cells. *Eur J Neurosci* **11:** 740–744

Kirsch J, Betz H (1995) The postsynaptic localization of the glycine receptor-associated protein gephyrin is regulated by the cytoskeleton. *J Neurosci* **15:** 4148–4156

Kirsch J, Betz H (1998) Glycine-receptor activation is required for receptor clustering in spinal neurons. *Nature* **392:** 717–720

Kirsch J, Kuhse J, Betz H (1995) Targeting of glycine receptor subunits to gephyrin-rich domains in transfected human embryonic kidney cells. *Mol Cell Neurosci* **6:** 450–461

Kirsch J, Langosch D, Prior P, Littauer UZ, Schmitt B, Betz H (1991) The 93-kDa glycine receptor-associated protein binds to tubulin. *J Biol Chem* **266:** 22242–22245

Kirsch J, Wolters I, Triller A, Betz H (1993) Gephyrin antisense oligonucleotides prevent glycine receptor clustering in spinal neurons. *Nature* **366:** 745–748

Kneussel M, Betz H (2000) Clustering of inhibitory neurotransmitter receptors at developing postsynaptic sites: the membrane activation model. *Trends Neurosci* **23:** 429–435

Kneussel M, Brandstatter JH, Laube B, Stahl S, Muller U, Betz H (1999a) Loss of postsynaptic GABA(A) receptor clustering in gephyrin-deficient mice. *J Neurosci* **19:** 9289–9297

Kneussel M, Hermann A, Kirsch J, Betz H (1999b) Hydrophobic interactions mediate binding of the glycine receptor beta-subunit to gephyrin. *J Neurochem* **72:** 1323–1326

Laskowsky RA, McArthur MW, Moss DS, Thornton JM (1993) PROCHECK: a program to check the stereochemical quality of protein structures. *J Appl Crystallogr* **276:** 307–326

Levi S, Vannier C, Triller A (1998) Strychnine-sensitive stabilization of postsynaptic glycine receptor clusters. *J Cell Sci* **111:** 335–345

Liu MT, Wuebbens MM, Rajagopalan KV, Schindelin H. (2000) Crystal structure of the gephyrin-related molybdenum cofactor biosynthesis protein MogA from *Escherichia coli*. *J Biol Chem* **275:** 1814–1822

Mammoto A, Sasaki T, Asakura T, Hotta I, Imamura H, Takahashi K, Matsuura Y, Shirao T, Takai Y (1998) Interactions of debrin and gephyrin with profilin. *Biochem Biophys Res Commun* **243:** 86–89

Meier J, De-Chaldee M, Triller A, Vannier C (2000) Functional heterogeneity of gephyrins. *Mol Cell Neurosci* **16:** 566–577

Meier J, Grantyn R (2004) A gephyrin-related mechanism restraining glycine receptor anchoring at GABAergic synapses. *J Neurosci* **24:** 1398–1405

Meier J, Vannier C, Serge A, Triller A, Choquet D (2001) Fast and reversible trapping of surface glycine receptors by gephyrin. *Nat Neurosci* **4:** 253–260

Meyer G, Kirsch J, Betz H, Langosch D (1995) Identification of a gephyrin binding motif on the glycine receptor beta subunit. *Neuron* **15:** 563–572

Moss SJ, Smart TG (2001) Constructing inhibitory synapses. *Nat Rev Neurosci* **2:** 240–250

Nooren IMA, Thornton JM (2003) Structural characterisation and functional significance of transient protein–protein interactions. *J Mol Biol* **325:** 991–1018

Nusser Z, Hajos N, Somogyi P, Mody I (1998) Increased number of synaptic GABA(A) receptors underlies potentiation at hippocampal inhibitory synapses. *Nature* **395:** 172–177

Prior P, Schmitt B, Grenningloh G, Pribilla I, Multhaup G, Beyreuther K, Maulet Y, Werner P, Langosch D, Kirsch J, Betz H (1992) Primary structure and alternative splice variants of gephyrin, a putative glycine receptor–tubulin linker protein. *Neuron* **8:** 1161–1170

Rees MI, Harvey K, Ward H, White JH, Evans LI, Duguid IC, Hsu CC, Coleman SL, Miller J, Baer K, Waldvogel MF, Gibbon F, Smart TG, Owen MF, Harvey RF, Snell RG (2003) Isoform heterogeneity of the human gephyrin gene (GPHN), binding domains to the glycine receptor and mutation analysis in hyperekplexia. *J Biol Chem* **278:** 24688–24696

Rosenberg M, Meier J, Triller A, Vannier C (2001) Dynamics of glycine receptor insertion in the neuronal plasma membrane. *J Neurosci* **21:** 5036–5044

Schmitt B, Knaus P, Becker CM, Betz H (1987) The Mr 93 000 polypeptide of the postsynaptic glycine receptor complex is a peripheral membrane protein. *Biochemistry* **26:** 805–811

Schrader N, Kim EY, Winking J, Paulukat J, Schindelin H, Schwarz G (2004) Biochemical characterization of the high affinity binding between the glycine receptor and gephyrin. *J Biol Chem* **279:** 18733–18741

Schwarz G, Schulze J, Bittner F, Eilers T, Kuper J, Bollmann G, Nerlich A, Brinkmann H, Mendel RR (2000) The molybdenum cofactor biosynthetic protein Cnx1 complements molybdate-repairable mutants, transfers molybdenum to the metal binding pterin, and is associated with the cytoskeleton. *Plant Cell* **12:** 2455–2472

Sola M, Kneussel M, Heck I S, Betz H, Weissenhorn W (2001) X-ray crystal structure of the trimeric N-terminal domain of gephyrin. *J Biol Chem* **276:** 25294–25301

Stallmeyer B, Schwarz G, Schulze J, Nerlich A, Reiss J, Kirsch J, Mendel RR (1999) The neurotransmitter receptor-anchoring protein gephyrin reconstitutes molybdenum cofactor biosynthesis in bacteria, plants, and mammalian cells. *Proc Natl Acad Sci USA* **96:** 1333–1338

Xiang S, Nichols J, Rajagopalan KV, Schindelin H (2001) The crystal structure of *Escherichia coli* MoeA and its relationship to the multifunctional protein gephyrin. *Structure* **9:** 299–310